

MORPHOLOGICAL AND STRUCTURAL FEATURES OF CO/TiO₂ CATALYSTS PREPARED BY DIFFERENT METHODS AND THEIR PERFORMANCE IN THE LIQUID PHASE HYDROGENATION OF α , β UNSATURATED ALDEHYDES

M. C. AGUIRRE ⁽¹⁾, G. SANTORI ⁽²⁾, O. FERRETTI ⁽²⁾, J. L. G. FIERRO ⁽³⁾, P. REYES ⁽¹⁾,

⁽¹⁾Departamento de Físico-Química, Facultad de Ciencias Químicas, Universidad de Concepción, Casilla 160-C, Concepción, Chile.

⁽²⁾ CINDECA (UNLP-CONICET), 47 N° 257, 1900 La Plata, Argentine.

⁽³⁾ Instituto de Catálisis y Petroleoquímica, CSIC, Cantoblanco, 28049 Madrid, Spain

ABSTRACT

The effect of the preparation method of Co/TiO₂ catalysts on the performance in the liquid phase hydrogenation of cinnamaldehyde and crotonaldehyde has been studied. The Co/TiO₂ catalysts were prepared by impregnation on titania (TiO₂, P-25), sol-gel, and precipitation procedures. Different reduction-oxidation-reduction cycles were carried out in order to detect possible changes in the nature of the phases and their reduction degrees. The catalysts were characterized by specific area measurements, TEM, ED, XPS and TPR/TPO studies. The catalysts prepared by the sol-gel and precipitation method exhibit higher resistance to sintering when they are treated under the same reduction-oxidation-reduction cycles, than the impregnated catalyst. Morphological changes observed by TEM were used to explain the catalytic behavior showed by the catalysts. The presence of Co⁰, CoO and Co₃O₄ phases in the reduced samples were detected by different methods. XPS results show the existence of small particles of CoO, which are interacting with the support, which are very difficult to reduce. TEM and electron diffraction structural studies show an effect of metal-support interaction by the appearance of channels and pill-box form in the particles. The highest yield in both catalytic hydrogenation reactions were obtained with the Co/TiO₂ catalysts prepared by precipitation and sol gel methods. The selectivity was closed to 50 and 30 % for cinnamyl alcohol and crotyl alcohol, respectively.

Keywords: Co/TiO₂ catalysts, characterisation, hydrogenation, cinnamaldehyde, crotonaldehyde.

INTRODUCTION

The selective hydrogenation of α , β unsaturated aldehydes to produce unsaturated alcohols is of great importance in the area of fine chemicals ^{1,2}. It has been reported that certain metals ³ are able to improve the selectivity to the alcohols due to they may reduce selectively the C=O bond. An increase in the metal particle size ⁴, effect of porosity of the support ⁵ and metal-support interactions ⁶ can enhance the selectivity to unsaturated alcohol. Several studies using Co as catalysts have shown good performance in the studied reaction. Miura et al.⁷, have reported the selective hydrogenation of different α , β unsaturated aldehydes in liquid phase over Co/Al₂O₃. They showed that the substitution in the δ position (specifically more voluminous groups) was more effective than in the α position to the formation of unsaturated alcohol. Nitta et al.⁸, have pointed out the importance of the preparation method and pretreatment conditions of Co catalysts on the selectivity of cinnamaldehyde and crotonaldehyde hydrogenation. Imanaka et al.⁹ have also studied the selective hydrogenation of cinnamaldehyde and crotonaldehyde over Co/SiO₂ catalysts. The structure sensitivity is explained in terms of strength of adsorption and the high

selectivity is related with large particle sizes. The effect of metal-support interaction in titania-supported catalysts during the liquid phase hydrogenation of unsaturated aldehydes has been explained by several authors ¹⁰. The use of Pt-Sn, Pt-Fe catalysts, has demonstrated that the support effect could be combined with the bimetallic effect to obtain higher selectivities and activities. Claus et al. ¹¹, working with Pt/TiO₂ catalysts prepared by impregnation and sol gel methods have reported the influence of the phase composition of titania on the activity and intramolecular selectivity in the liquid phase hydrogenation of crotonaldehyde.

The objective of this work is to study the effect of different preparation methods of Co/TiO₂ catalysts on the catalytic behavior in the hydrogenation of cinnamaldehyde and crotonaldehyde in liquid phase. The identification of different active sites by the diffraction electron technique and the metal-support interactions as well as changes, in the morphology as a function of the reduction degree, were observed by TEM. The identification of the different oxidation states and morphologies of cobalt species provides support to explain the observed catalytic behaviour.

EXPERIMENTAL SECTION

Co/TiO₂ catalysts were prepared by impregnation of titania (P-25, Degussa), sol-gel and alkaline precipitation methods, using an acetone solution of cobalt acetylacetonate in the appropriate amount to obtain 5 wt % of the metal. In the first method, the support was previously calcined in air at different temperatures: 673, 873, 973 and 1073 K for 5 h. The prepared supports were contacted in a rotary evaporator with a metallic precursor solution under continuous stirring at 308 K during 5 h.. The catalysts were labelled as: Co/TiO_{2 (673)}-I, Co/TiO_{2 (873)}-I, Co/TiO_{2 (973)}-I and Co/TiO_{2 (1073)}-I.

The sol gel catalyst was prepared in a reactant mixture of tetraethoxy titanium, ethanol, and cobalt acetylacetonate in acetone solution and kept under reflux and continuous stirring at 343 K during 24 h. The hydrolysis was accelerated by dripping water during 2 h up to reach a water/alkoxide molar ratio of 7. The catalyst was labelled as: Co/TiO_{2 (673)}-SG.

In the third preparation procedure, the metal component was precipitated by the addition of an excess of alkaline base (KOH), over a fine dispersion of the support in an acetone solution of the metal precursor. The mixture was stirred under reflux at 373 K during 4 h. Then, it was filtered and washed thoroughly with bidistilled water at 373 K until the filtered solution reached a pH 7. The catalyst was labelled as: Co/TiO_{2 (673)}-P. All the samples prepared by different methods were dried at 383 K for 12 h and calcined at 673 K for 4 h. Then they were reduced *in situ* prior to their characterisation or catalytic tests.

The specific surface area of the support was evaluated from nitrogen adsorption isotherm at 77 K determined in a Micromeritics Model ASAP 2010. Temperature programmed reduction and oxidation studies, TPR/TPO, were carried out in a TPD/TPR 2900 Micromeritics using a mixture of 5% H₂/Ar (50 cc/min) and a heating rate of 10 °/min. Cycles of reduction-oxidation-reduction (TPR-TPO-TPR) at high temperatures (773-623 -773 K) and at low temperatures (623 -623 -623 K) were carried. Reduction cycles at (1073-1073-1073 K) were also used.

Transmission electron micrographs and electron diffraction patterns were obtained with a Jeol JEM 1200 EXII microscope. The supported catalysts were ground in an agate mortar and dispersed in ethanol. A drop of each dispersion was placed on a 150 mesh copper grid coated with carbon. to evaluate the metal particle size, several magnifications were used in both bright and dark fields. For electron diffraction studies 120 kV and 60 cm were used as acceleration voltage and focus distance respectively and a gold standard (Merck 99.99% pure) was used for calibration. XPS spectra were recorded using a VG Escalab 200R spectrometer equipped with a hemispherical electron analyser and a Mg K_α X-ray source (hν = 1253.6 eV). The system was provided with a reaction cell which allows pretreatment at

high temperatures. The samples were pressed in a hydraulic die to form thin, smooth discs and placed in the cell. The samples were pretreated following the reduction-oxidation-reduction cycle at 773 K/1h- 623 K/0.5 h-773 K/1 h, and then transported to the analysis chamber without contact with air. Co peaks were decomposed into several components assuming that the peaks had Gaussian-Lorentzian shapes. Surface Co/Ti and was estimated from the integrated intensities of Co 2p_{3/2}, and Ti 2p_{3/2} lines after background subtraction and corrected by the atomic sensitivity factors¹². The C 1s core-level of adventitious carbon at a binding energy (BE) of 284.9 eV was taken as an internal standard.

The metallic content was analysed by Atomic Absorption using IL 457 equipment (wavelength 240.7 nm, acetylene-air flame). In all the cases the experimental Co content were closed to the nominal values.

X-ray diffraction of calcined support and reduced catalysts were obtained with Rigaku diffractometer using Ni filter, Cu Kα± radiation, (λ= 1.5418Å).

The catalytic reactions were carried out in a stirred batch reactor at 15 atm of hydrogen pressure. The reduced catalyst (0.5 g) was added to the reactor and mixed with 80 mL of a 0.15 M solution of crotonaldehyde in isopropanol (or cinnamaldehyde in toluene). The reaction temperature was 313 K (or 358 K) for crotonaldehyde (or cinnamaldehyde) hydrogenation, respectively. The analyses of reactants and products were performed using a Varian 3400 gas chromatograph equipped with a 30m J&W DB-WAX capillary column and a flame ionisation detector.

RESULTS AND DISCUSSION

The effect of the preparation method on the specific area, metal particle size, metallic dispersion and reduction degree are compiled in Table I. The specific surface area at the same calcination temperature, 673 K is higher in the catalysts prepared by the sol-gel procedure compared with those obtained by precipitation or impregnation of a commercial support. In this latter, a significant decrease in surface area is observed as the calcination temperature increases. This feature is accomplished by a change in the crystalline phases of the support as it has been demonstrated by XRD. In fact, in the Co/TiO_{2 (673)}-SG catalysts only anatase phase appears, whereas, both, anatase and rutile are present in the Co/TiO_{2 (673)}-P and Co/TiO_{2 (673)}-I catalysts. In both catalysts anatase is the major crystalline titania phase, being 2.94 the anatase/rutile ratio. In the impregnated series, the transformation anatase to rutile occurs upon increasing the calcination temperature, being only rutile the phase observed when the support calcination is 1073 K. On the other hand, TEM was used to evaluate the metal particle size of samples upon the reduction-calcination-reduction cycle. After final reduction at

Table I Specific area, anatase/rutile ratio (A/R), metal particle size by TEM and Cobalt dispersion of Co/TiO₂ catalysts

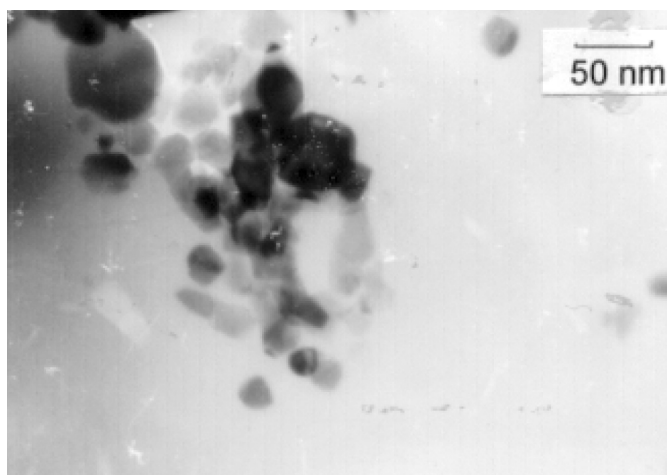
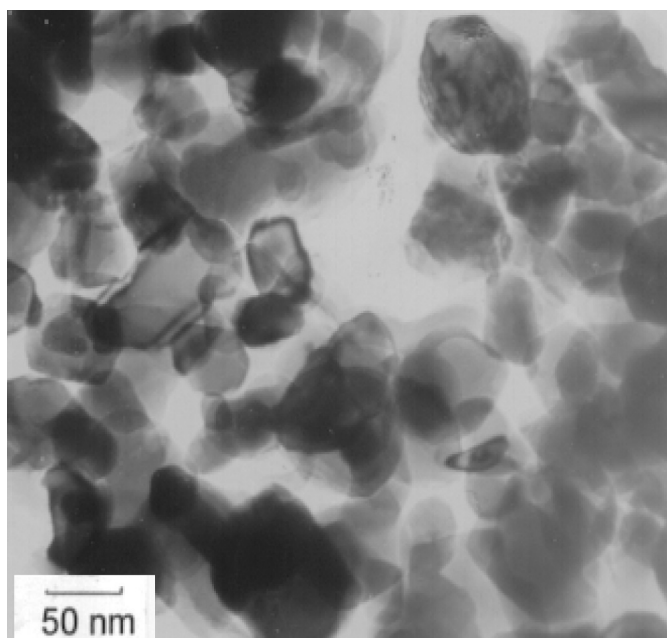
Catalyst	S _{BET} m ² /g	A/R	TEM		D(%)	
			623 K*	773 K**	623K*	773 K**
Co/TiO ₂₍₆₇₃₎ -I	50	2.94	2.7	16	35	6
Co/TiO ₂₍₈₇₃₎ -I	48	1.66	4	21	24	4
Co/TiO ₂₍₉₇₃₎ -I	20	0.13	3.3	20	29	5
Co/TiO ₂₍₁₀₇₃₎ -I	13	0	9	21	11	4
Co/TiO ₂ -SG ₍₆₇₃₎	81	100/0	2.7	3.1	35	31
Co/TiO ₂₍₆₇₃₎ -P	61	2.94	3.2	3.3	30	29

* Cycle 773-623-623 K

** Cycle 773-623-773 K

623 K, the cobalt particle size were in the range 2.7-4.0 nm in most of the studied catalysts, being the only exception the sample prepared by impregnation. A significant enhancement in the cobalt particle size is obtained in the impregnated samples if the reduction-oxidation-reduction cycle is completed with a reduction in hydrogen at higher temperature (773 K). However, no significant changes were observed in those obtained by precipitation or sol-gel. This behaviour may be explained on the basis of a stronger interaction between the support and cobalt in the precipitated and sol-gel that makes the metal particles more resistance to sintering compared with the impregnated catalysts. Table I also compiles the metal dispersion determined from TEM data by using the Reul and Bartholomew¹³ equation, D(%) = 96/d (nm). This method has the advantage to give more realistic metal dispersion values compared with those obtained from H₂ chemisorption because H₂ adsorption is drastically suppressed in the presence of titania-support that becomes partially reduced. High cobalt dispersion, close to 30%, was obtained upon the reduction-oxidation-reduction cycle at low temperatures. On the contrary, dispersion around 5% was determined for the impregnated samples treated under to the high temperature reduction cycle.

The preparation method may also involves significant changes in the particle morphology and the form of the insertion of the metal to the support in a sol-gel and precipitated catalysts, being different in those catalysts prepared by the impregnation procedure. The micrograph of a Co/TiO₂₍₆₇₃₎-I catalyst after a reduction-oxidation-reduction cycle at 623 K (Fig. 1) shows a pill-box morphology. When the impregnated catalysts are treated at the high temperature cycle (773 K), not only changes in the particle size but also other important morphology changes occur. In fact, after this treatment the cobalt species are present as thin crystals. In general, the changes in the morphology and size in the impregnated Co/TiO₂ series were more significant when the calcination temperature of the support was higher. Figure 2 shows a micrograph of a Co/TiO₂₍₉₇₃₎-I catalyst after the 773-623-773 K cycle. A well-defined thin oxide layers covered by a metallic

**Figure 1.** TEM micrograph, of Co/TiO₂₍₆₇₃₎-I catalyst after reduction-oxidation-reduction cycle at 773-623-623 K.**Figure 2.** TEM micrograph, of Co/TiO₂₍₉₇₃₎-I catalyst after reduction-oxidation-reduction cycle at 773-623-773 K.

kernel can be observed. On the other hand, practically no changes in the cobalt particle size was observed in the $\text{Co}/\text{TiO}_{2(673)}\text{-SG}$ catalysts after the cycles at low or high temperature, as it is illustrated in Fig. 3. This behaviour can be explained assuming that during the preparation of the catalyst, the cobalt precursor species were highly dispersed in the titania network and consequently, a very narrow particle size distribution of small particle size is observed for this catalyst. Conversely, in the

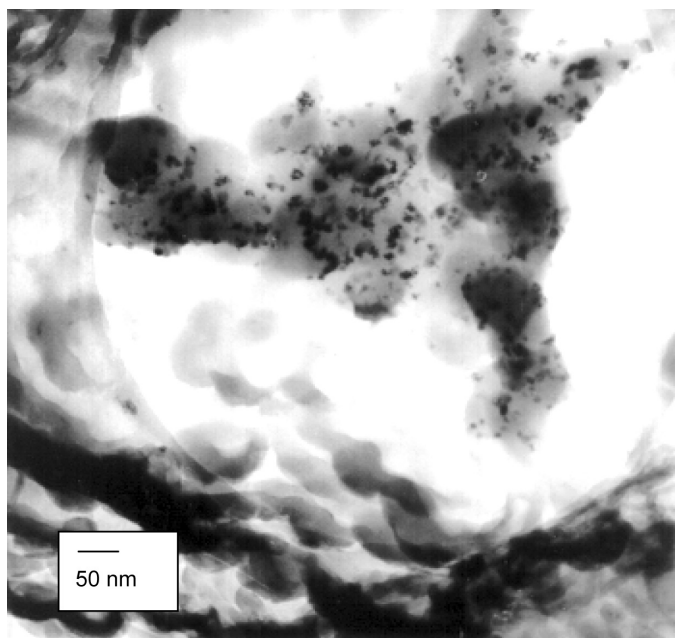


Figure 3. TEM micrograph, of $\text{Co}/\text{TiO}_{2(673)}\text{-SG}$ catalyst after reduction-oxidation-reduction cycle at 773-623-773 K

precipitated catalyst the micrograph evidences the presence of channelling or Moiré fringes lines indicating that, under these conditions, there exists diffusion of TiO_x moieties towards metallic sites. The formation of “Moiré fringes” with different intensities stands out the changes in the geometry of the particle¹⁴.

The irregularities in the spacing and intensities showed in the micrograph (Fig. 2), suggest modification in the particles composition due to the different states of the reduction of cobalt ions. X-ray diffraction data indicate a low quantity of the Co oxides in crystalline state after calcination, which have a well defined and specific morphology. Taking into account that Co_3O_4 can be easily reduced, it would be covered by CoO species which are in more intimate contact with the support and, therefore, they are more difficult to reduce. Due to the presence of the different oxidation states of cobalt, irregular growing of the particles in the impregnated catalysts would be possible and a pseudomorphism is suggested, existing strong interactions between the metal and support. Dumesic et.al¹⁵ have reported morphological changes with the reduction temperature in Fe/

TiO_2 catalysts prepared by chemical vapour deposition technique. The nucleation of the Fe overlays in three-dimensional crystallites at temperatures as low as 707 K, and diffusion of Fe in TiO_x at higher reduction temperatures. In our case, the electron diffraction technique was an appropriate technique to provide information about the different cobalt species. Co species in the samples were better identified in the bulk of the particles.

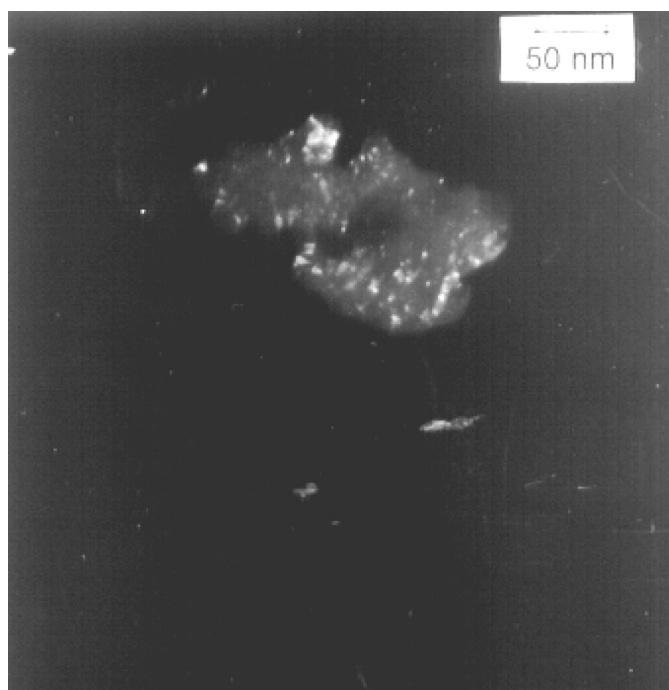


Figure 4. (A), Electron diffraction pattern of $\text{Co}/\text{TiO}_{2(973)}\text{-P}$ catalyst after reduction-oxidation-reduction cycle at 773-623-773 K. (B), TEM micrograph of the first ring of the diffraction. (C), TEM micrograph, of the zone diffracted of $\text{Co}/\text{TiO}_{2(973)}\text{-P}$ catalyst after reduction-oxidation-reduction cycle at 773-623-773 K.

Figure 4a shows the electron diffraction of the $\text{Co}/\text{TiO}_{2(673)}\text{-P}$ catalyst, after the reduction cycle at 773 K. It shows the characteristic auto hexagonal lines of a face cubic centred crystal, with the main planes of Co_3O_4 (fcc), Co (fcc) and $\alpha\text{-Co}^0$ (hex.). The more intense lines correspond to (220) plane of Co_3O_4 with $d_{(hkl)}$ of 2.86 Å and the (311) plane with $d_{(hkl)}$ of 2.43 Å. In the third ring, the sequence of cubic Co^0 to $d_{(hkl)}$ nearly at 2 Å would be considered. The fourth well defined ring, can be assigned to the face (200) of Co^0 with a $d_{(hkl)}$ of 1.77 Å. Although it has been reported in literature¹⁶ that this phase can only be formed at high temperatures, diffraction lines of striking intensities as corresponding at $d_{(hkl)}$ of 1.77 Å were observed in this sample. In spite of the cubic centred face, the presence of hexagonal $\alpha\text{-Co}^0$ can not be neglected because of the metallic Co phase is more likely to be formed at room temperature. The micrograph of the first and second diffraction rings shows an uniform particle size distribution centred around 2 nm which corresponds to Co_3O_4

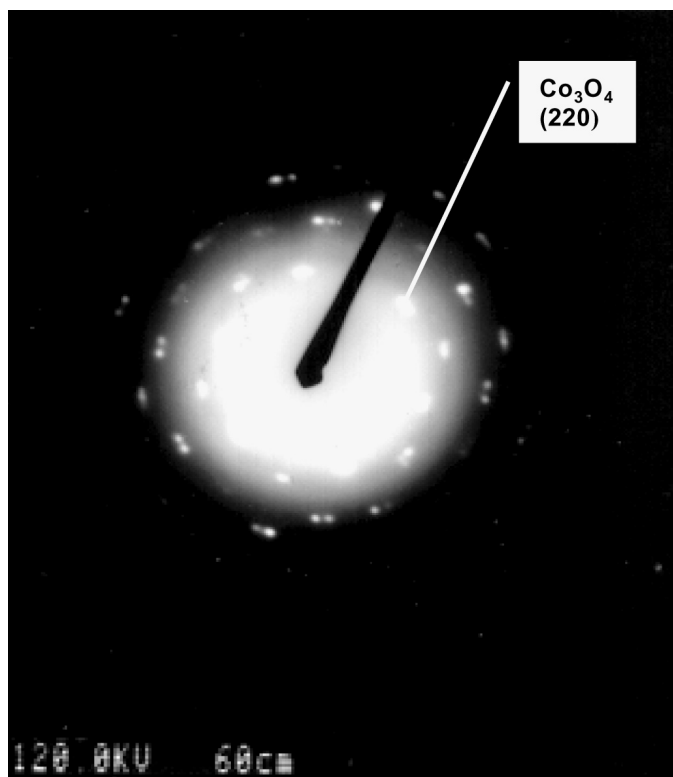


Figure 4b



Figure 4c

crystals with (220) and (311) planes, (see Fig. 4b). The channelling showed in Fig 4c indicates diffusion of TiO_x species to the metallic sites, which partially cover the small particles observed in the diffracted area. On the other hand, the electron diffraction of representative samples of impregnated series, showed a crystalline material with a diversity of phases corresponding to the different reduction states of cobalt and TiO_2 . The spot analysis indicated changes in the crystallinity of the different catalysts according to the degree of reduction as shown by TPR profiles. Those samples with lower specific area displayed less diffracted planes, confirming the idea of the major formation of amorphous oxide layers.

The impregnated samples showed mainly the presence of Co_3O_4 and Co^0 lines in a cubic symmetry. Metal cobalt particles are possibly favoured in reducible supports at high reduction temperatures (higher than 773 K). The deformation of the rings in the micrograph (quasi-elliptic shape) evidence the SMSI effect discussed previously. The presence of diffraction lines of the support, corresponding mainly to the rutile phase in all the catalysts of the impregnated series, suggests a transformation anatase to rutile during the reduction process. It is likely that the reduction enhances the compaction of the support. During the

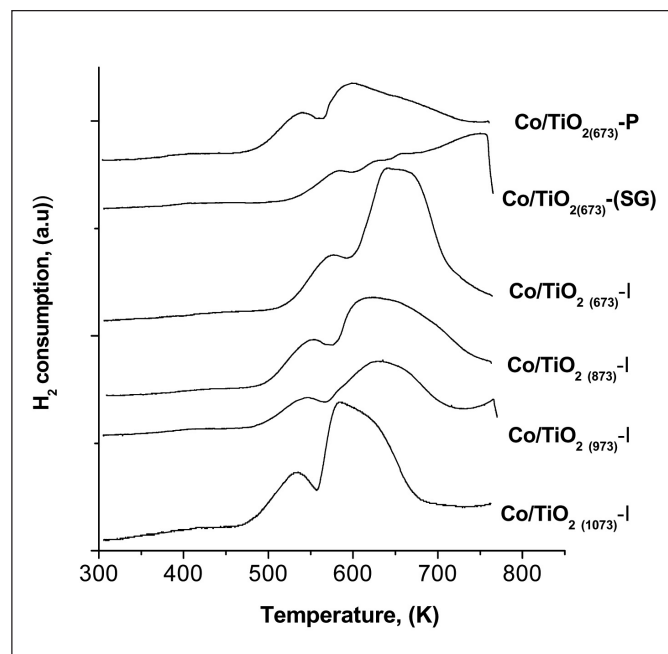
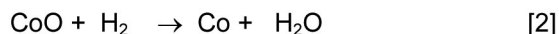
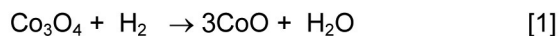


Figure 5. Temperature-programmed profile of Co/TiO_2 catalysts after reduction-oxidation-reduction cycle at 773-623-773 K.

reduction, new shear phases are created, which restrict the diffusion of O^{2-} , and H_2O in a minor degree. The diffusion through to the shear planes is difficult due to a high packing of ions in these layers. The existence of the shear planes in the rutile-type structure makes the dissociation of H_2 difficult, inhibiting the reduction of the metal and it is responsible of the lower

reducibility of the metal in the impregnated series when the anatase/rutile ratio decreased.

Temperature-programmed reduction profiles of Co/TiO₂ samples are shown in Fig. 5. The profiles correspond to the reduction of the samples after reduction at 773 K in H₂ followed by oxidation at 623 K for 30 min. Two reduction steps are clearly identified. The first peak centred at about 570 K may be attributed to the reduction of Co₃O₄ to CoO whereas the second, close to 630 K, should be associated to further reduction to Co⁰, according to the following scheme:



The extent of reduction of cobalt oxides was obtained assuming the previous scheme, showing that in all the samples no complete reduction was achieved. Comparing the experimental H₂ consumption with the theoretical one, the reduction degree is in the range 50 to 80%. Although all the samples exhibited H₂ consumptions higher than the required to accomplish a complete transformation of Co₃O₄ to CoO, the stepwise reduction of Co₃O₄ to Co⁰ in a single step for Co₃O₄ species, placed on top of metallic Co, can not be neglected. Slight shifts in the reduction temperature were detected in both steps for the different catalysts. Thus, the reduction peaks in Co/TiO₂₍₆₇₃₎-P sample are centred at 530 and 580 K, nearly 40 K lower than in the impregnated counterparts. These changes may be attributed to a more intimate metal-support contact in the former that makes easier the formation of Co⁰ nucleus, by an assisted reduction of other Co₃O₄ or CoO particles. In the Co/TiO₂₍₆₇₃₎-SG, even the reduction peaks are placed at comparable temperatures than the impregnated series, it shows a lower reduction degree. This result is attributed to the insertion of Co species in the titania lattice during gelation and, therefore, its reduction is more difficult. Besides, in the impregnated series an increase in the proportion of rutile, leads to a higher compaction of the support and to a higher cobalt particle size. The reduction of these larger crystals can be reasonably described by the sphere-contraction model¹⁷. Thus, after the formation of a metallic shell of cobalt, the reduction rate drops because of diffusional restriction of H₂ to access to inner sites of the particles and also by the evolution of water formed during reduction. It should also be mentioned that, during the oxidation step, the presence of oxygen allows the oxidation of the reduced species and also improves the dispersion of the larger cobalt oxide crystals. Therefore, in the following reduction step (second TPR), the reduction degree increases significantly and shifted the maximum of reduction at lower temperatures, whereas a thin layer of cobalt oxide-Co⁰ is formed. Reduction cycle (773-623 - 773 K) did not show an increase in the reduction degree, due to the appearance of new phases formed during the oxidation step. It is assumed that the oxidation at high temperature makes possible the formation of cobalt titanate. Dumesic et al.¹⁸ have

reported that Fe/TiO₂ catalysts reduced at high temperature (979 K) lead to a FeTi₂O₃ phase by the diffusion of the Fe²⁺ ions into the support.

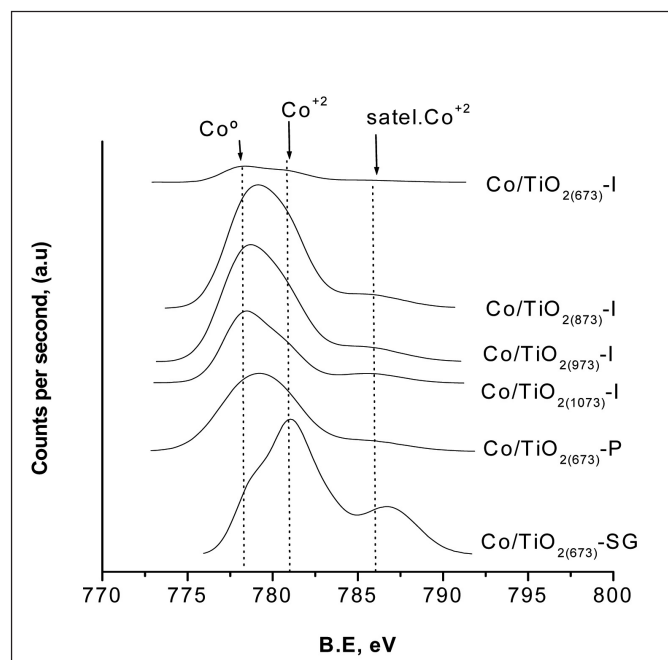


Figure 6. Co 2p_{3/2} core-level spectra of Co/TiO₂

Figure 6 shows the X-ray photoelectron spectra of Co 2p_{3/2} core-level of the reduced catalysts. The BE of the Co 2p_{3/2} peak at ca. 780.6-781.0 eV corresponds to Co²⁺ species, which is also in agreement with the observation of its satellite line at 786.9 eV in these Co/TiO₂ catalysts. However, the lower intensity of the satellite peak observed in the samples with lower specific area would be considered as indicative of the presence of a minor proportion of Co³⁺ species (at 779 eV). Co⁰ having the Co 2p_{3/2} peak at 778.2 eV was detected in all the samples. It is likely that clusters of only a few Co⁰ atoms lead to a shift in the BE towards higher values and, therefore, it behaves close to the Co²⁺ species. The BE values and Co/Ti atomic surface ratios of the samples after the reduction cycle (773-623-773 K) are compiled in Table II. A good relationship between the BE of Co 2p_{3/2} core-level and the preparation treatments were obtained, revealing that the Co²⁺ environment changes in the different samples. In fact, in the impregnated catalysts series, the decrease in the intensity of the Co²⁺ satellite peak, as the calcination temperature of the support increases, suggest the presence of Co³⁺ surface species, and are accompanied by an important enhancement in the surface Co/Ti ratio. This feature is also supported by the lower specific area exhibited by the support calcined at higher temperatures. The observed drop in the intensity of Co 2p_{3/2} peak run in parallel with the shift in the maximum of BE from 780.0 eV to 779.0 eV in the sample Co/TiO₂₍₁₀₇₃₎-I. The signal of octahedral coordinated Co³⁺ of Co₃O₄ is even more evident in Co/TiO₂₍₉₇₃₎-I and Co/

Table II. Binding energies (eV) of core-levels, surface ratios and reduction degree (%R)

Catalyst	B. E. eV O 1 s	B.E. eV Co 2p _{3/2}	B.E. eV Ti 2p _{3/2}	(Co/Ti) _s	% R
Co/TiO ₂ (₆₇₃)-I	529.8 (79) 531.3 (21)	778.1 (40) 780.6 (60)	458.5	0.190	79
Co/TiO ₂ (₈₇₃)-I	529.8 (86) 531.5 (14)	778.3 (53) 780.1 (47)	458.6	0.193	78
Co/TiO ₂ (₉₇₃)-I	529.8 (82) 531.6 (18)	778.2 (51) 780.6 (49)	458.4	0.228	57
Co/TiO ₂ (₁₀₇₃)-I	529.8 (82) 531.5 (18)	778.2 (61) 780.6 (39)	458.4	0.880	57
Co/TiO ₂ (₆₇₃)-SG	529.8 (78) 531.3 (22)	778.2 (45) 780.5 (55)	458.5	0.550	61
Co/TiO ₂ (₆₇₃)-P	529.8 (81) 531.4 (19)	778.3 (49) 780.3 (51)	458.5	0.330	67

TiO₂(₁₀₇₃)-I catalysts. The change in the intensity of the satellite peak can also be attributed to a higher proportion of tetrahedral than octahedral Co⁺² phases. A higher extent of the tetrahedral phase induces an increase in the intensity of the satellite peak if different phases of the cobalt (or cobalt oxides) are present. XPS studies of CuO/Cr₂O₃ catalysts¹⁹ showed CuO and CuCr₂O₄ separated phases (the first octahedral and the second tetrahedral). For this system, an increase in the intensity of the satellite peak when CuCr₂O₄ phase is present in a higher proportion was reported¹⁹.

On the other hand, Co/TiO₂(₆₇₃)-P and Co/TiO₂(₆₇₃)-SG catalysts showed the signal arising from surface Co⁰, although, taking into account the preparation route, is likely that small CoO species remains in strong interaction with the titania. This may explain the difficulty in the reduction of cobalt ions in these samples. An increase in the intensity of the satellite peak at 787 eV on the Co/TiO₂(₆₇₃)-SG catalysts compared to the impregnated and precipitated catalysts would be interpreted as due to a strong interaction of cobalt with titania during the gelation process, in spite of Co⁺² species are mainly in tetrahedral coordination.

The O 1s core-level peaks at 529.8 and 531.5 eV are attributed to O 1s of Ti-O-Ti and Ti-OH bonds²⁰ whereas Ti 2p_{3/2} level exhibits only one component centred at 458.5 eV, assigned to Ti⁺⁴ species. The presence of Ti⁺³ species, in a very low proportion, cannot be detected under the used conditions. However, this reduction should be confined in local regions of the support near or below the cobalt crystallites making more difficult its detection. Additionally, only small islands of titanium suboxides would be covering the metallic particle, which would explain the absence of the signals of Co⁰. Bearing in mind the main characteristics showed in the micrographs, a gradual diffusion of Co into the support may lead to the formation of thin cobalt crystals. Similarly, Dumesic et al.²¹ have reported XPS studies of Fe/TiO₂ prepared by chemical vapour deposition technique. They found that after reduction at 773 K the smaller iron crystallites can diffuse into the support, which suggests a partial reduction of the titania, however, only Ti⁺⁴ species were detected in agreement with our findings.

Table III, summarises the results of cinnamaldehyde hydrogenation at 358 K on the Co/TiO₂ catalysts after a higher

Table III. Reaction rate and unsaturated alcohol yield for cinnamaldehyde hydrogenation

Catalyst	Rate reaction μmole/gcat.min	Yield cinnamyl alcohol, μmole/gcat.min, 10 ⁻²
Co/TiO ₂ (₆₇₃)-I*	11.8	436
Co/TiO ₂ (₆₇₃)-I	16.5	643
Co/TiO ₂ (₈₇₃)-I	19.4	718
Co/TiO ₂ (₉₇₃)-I	15.7	549
Co/TiO ₂ (₁₀₇₃)-I	14.0	518
Co/TiO ₂ (₆₇₃)-SG	21.9	876
Co/TiO ₂ (₆₇₃)-P	23.8	785

*623-623-623

temperature reduction cycle (773-623-773). The reaction rate and cinnamyl alcohol yield were evaluated in the low conversion range from 0 to 10%, and they were expressed as μmol of unsaturated aldehyde or alcohol by gram of catalyst and minute. The reaction rate indicated to be of zero order with respect to cinnamaldehyde concentration. As it can be seen, the highest yielded of alcohol are displayed by the $\text{Co}/\text{TiO}_{2(673)}\text{-P}$ or sol-gel catalysts which possess the higher cobalt dispersion, and almost no change in the particle size with the reduction cycle. However, looking at the impregnated series the behaviour seems to be different. In fact, an increasing in the calcination temperature of the support leads to a decrease in the specific area, in parallel to a drop in the anatase/rutile ratio and the yield displays a maximum in the $\text{Co}/\text{TiO}_{2(873)}\text{-I}$ catalyst.

This behaviour indicates that not only the particle size has an impact on the activity but also the morphology of the particle and the environment of the metallic cobalt. In fact, different authors have reported that the cinnamaldehyde hydrogenation may be considered as a structure-sensitive reaction and that a better performance is achieved in the catalysts having larger particles due to steric hindrance for the $\text{C}=\text{C}$ adsorption on flat surfaces. Consequently, catalysts having higher particle sizes are expected to display a higher activity. However, this trend does not fit in the $\text{Co}/\text{TiO}_{2(1073)}\text{-I}$ catalyst which possesses the largest particle size but does not show the highest yield. On the impregnated series, changes in the catalytic activity was

observed, even if the main difference is the calcination temperatures of the support, suggesting that different interfacial sites are created according to the anatase/rutile ratio. This interaction is also affected by the ratio $\text{Co}^{2+}/\text{Co}^{3+}$ and also by the changes in the reduction degree. In the impregnated series, the $\text{Co}/\text{TiO}_{2(873)}\text{-I}$ catalyst which showed the higher reduction degree leading to Co^0 species, was the only one that showed the highest yield. Similar results have been reported by Claus et al.¹¹ for Pt/TiO_2 system, in which an increase in the anatase fraction produces an important drop in the catalytic activity. This behaviour was attributed to changes in the competitive adsorption and readsorption of the products, which strongly depend on the TiO_2 phase composition. In the $\text{Co}/\text{TiO}_{2(673)}\text{-SG}$ catalyst, the possible substitution of the metal in the lattice²¹ may facilitate the strong metal-support interaction (SMSI), which improves the yield of the catalyst. In all catalysts an increase in the selectivity to saturated alcohol with the conversion has been observed whereas the selectivity to the saturated aldehyde diminishes and the selectivity of unsaturated alcohol remains approximately constant (c.a. 40 %).

Table IV shows the rate reaction and the yield to crotyl alcohol, during crotonaldehyde hydrogenation using $\text{Co}/\text{TiO}_{2(873)}\text{-I}$, $\text{Co}/\text{TiO}_{2(673)}\text{-P}$ and $\text{Co}/\text{TiO}_{2(673)}\text{-SG}$ as catalysts. As can be seen, $\text{Co}/\text{TiO}_{2(673)}\text{-SG}$ shows the highest yield. The catalyst of highest activity led to values of selectivity to crotyl alcohol in the order of 30 % at level of 20 % of conversion. There was an

Table IV. Reaction rate and unsaturated alcohol yield for crotonaldehyde hydrogenation

Catalyst	Rate reaction $\mu\text{mol}/\text{gcat}.\text{min}$	Yield unsaturated alcohol, $\mu\text{mol}/\text{gcat}.\text{min}, 10^{-2}$
$\text{Co}/\text{TiO}_{2(873)}\text{-I}$	8	200
$\text{Co}/\text{TiO}_{2(673)}\text{-SG}$	24	600
$\text{Co}/\text{TiO}_{2(673)}\text{-P}$	43	1300

increase in the selectivity with conversion. This finding may be indicative that the interface sites responsible for the production to crotyl alcohol are improved during the reaction. Taking into account the characterisation results, a remarkable difference in the composition of the metallic phase as the anatase/rutile ratio decreases and increases of Co oxide phases was observed. XPS and TEM studies showed essentially small particles of CoO that interact with the support, which would provide the Lewis acid functionality required for this reaction. On the other hand, the TPR/TPO, electron TEM and diffraction results revealed the presence of metallic Co, which creates interfacial sites with titanium sub-oxide. The migration of TiO_x species during the reduction at high temperature, which cover the metallic particles, provides the cationic sites required for the interaction with $\text{C}=\text{O}$

group of the crotonaldehyde molecule, leading to the anchorage of C on the metallic particle and O on the cationic sites. The intimate contact between the hydrogenating sites (metallic particles) and electrophilic sites (partially reduced metal oxides) are necessary for the formation of selective intermediate species. On the other hand, due to an incomplete reduction of the Co oxide, the remaining cationic species of Co would provide the Lewis acid sites for the adsorption of $\text{C}=\text{O}$.

CONCLUSIONS

The results showed that the method of preparation of Co/TiO_2 catalysts has influence catalytic properties during the hydrogenation of α , β unsaturated aldehydes. Thus, changes in

the reduction degree, morphology, and surface coverage, which depend on the catalyst architectures derived from the preparation method, are connected with the catalytic behaviour. Particularly, the insertion of Co ions in the titania lattice and the small Co crystals trapped into the porous structure, lead to an increase in the metal-support interaction in the catalyst obtained by the sol-gel method. The catalyst obtained by a precipitation procedure exhibited a similar behaviour but the impregnated counterpart showed differences in morphology as a consequence of its anatase/rutile ratio. Metallic Co, CoO and Co₃O₄ were detected by electron diffraction. XPS results showed the existence of small CoO particles in intimate contact with the support, which are hardly reduced. TEM and electron diffraction structural studies showed pill-box shaped particles as expected from the metal-support interaction. The best results in cinnamaldehyde hydrogenation reaction were obtained with the Co/TiO₂ catalyst prepared by precipitation, but in the crotonaldehyde hydrogenation the Co/TiO₂ catalyst prepared by sol gel method show the highest yield to crotyl alcohol. The partial reduction of the support can generate SMSI effect, creating TiO_x-Co moieties as well as the presence of Co cationic species, which provide Lewis acid sites, contributing to an enhancement in the polarisation of C=O. The presence of dual sites in these kinds of catalysts seems to be responsible of the preferential formation of crotyl alcohol.

ACKNOWLEDGMENTS

The authors thank CONICYT (FONDECYT grants 1980345 and 2990065) for financial support. We thank to Mr. R Alarcón and Mr. M. Oportus for their valuable help.

REFERENCES

- Vannice, M. A., *J. Mol. Catal.*, **1990**, 59, 165.
- Poltarzewski, Z.; Galvagno, S.; Pietropaolo, R.; Saiti, P., *J. Catal.* **1986**, 102, 190.
- Gallezot, P.; Richard, D. *Catal. Rev.-Sci. Eng.* **1998**, 40, 81.
- Giroir-Fendler, A.; Richard, D.; Gallezot, P. *Catal. Lett.* **1990**, 5, 175.
- Reyes, P.; Aguirre, M. del C.; Pecchi, G.; Fierro, J.L.G. *J. Mol. Catal. A: Chem.* **2000**, 164, 245.
- Dandekar, A.; Vannice, M. A. *J. Catal.* **1999**, 183, 344.
- Ando, C.; Kurokawa, H.; Miura, H. *Appl. Catal. A: General* **1999**, 185, L181.
- Nitta, Y.; Hiramatsu, Y.; Imanaka, T. *J. Catal.* **1990**, 126, 235.
- Nitta, Y.; Ueno, K.; Imanaka, T. *Appl. Catal.* **1989**, 56, 9.
- Da Silva, A.; Jordao, E.; Mendes, M.; Fouilloux, P. *Appl. Catal. A: General* **1997**, 148, 253.
- Claus, P.; Schimpt, S.; Schödel, R.; Kraak, P.; Mörke, W.; Hönicke, D. *Appl. Catal. A: General*, **1997**, 165, 429.
- Wagner, C.D.; Davis, L. E.; Zeller, M. V.; Taylor, J. A.; Raymond, R. H.; H. Gale, L. *Surf. Interf. Anal.* **1981**, 3, 211.
- Reuel, C.; Bartholomew, C., *J. Catal.* **1983**, 83, 107.
- Yacamán, J.; Avalos-Borja, M. *Catal. Rev.-Sci. Eng.* **1992**, 34(1 & 2), 55.
- Tatarchuk, B.; Dumesic, J. *J. Catal.* **1981**, 70, 308.
- Castner, D.; Watson, P.; Chan, I.Y. *J. Phys. Chem.* **1990**, 94, 819.
- Baiker, A.; Gasser, D.; Lenzner, J.; Reller, A.; Schlögl, R., *J. Catal.* **1990**, 126, 555.
- Tatarchuk, B.; Dumesic, J. *J. Catal.* **1981**, 70, 335.
- Severino, F.; Laine, J.; Fierro, J.L.G.; Lopez-Agudo, A. *J. Catal.* **1998**, 177, 82.
- Reyes, P.; Rojas, H.; Fierro, J.L.G., *J. Mol. Catal. A. Chemical* **2003**, 203, 203.
- Tatarchuk, B.; Dumesic, J. *J. Catal.* **1981**, 70, 323.
- López, T.; Bosch, P.; Morán, M.; Gómez, R. *J. Phys. Chem.* **1993**, 97, 1671.
- Luo, S.; Falconer, J.L. *Catal. Lett.* **1994**, 57, 335.

